Mohammed H. Al-Dharob [1]
Ammar A. Hamad [2]
Ahmed Y. Qasim [3]
Omar A. Abdulrazzaq [4]
Ahmed A. Alwan [4]

[1] *Al-Karkh University of Science, Baghdad, IRAQ*
[2] *Ministry of Industry and Minerals, Scientific Advisory Office, Baghdad, IRAQ*
[3] *Corporation of Research and Industrial Development, Baghdad, IRAQ*
[4] *Renewable Energy and Environment Research Center, Corporation of Research and Industrial Development, Baghdad, IRAQ*

Investigating the Potential of Al_2O_3 Nanocomposites for Innovative Self-cooling Photovoltaic Technology

In this research, we investigate the use of a passive radiative self-cooling layer made of an Al_2O_3 nanocomposite on the backside of a compact 10W PV module. The coating, composed of Al_2O_3 nanoparticles (with a particle size of 30nm) blended with $Na_2SiO_3.9H_2O$ in a specific ratio, forms a ceramic glue applied to the module's rear surface in both horizontal and vertical directions using a standard paintbrush. The experiments were carried out in the 50°C ambient temperature of Baghdad summer. The results indicate a significant decrease in the temperature of the PV module in hot weather, reducing from 63°C to 58°C with the application of the nanocomposite layer. Additionally, the nanocomposite coating improves key performance parameters, such as open circuit voltage, short circuit current, voltage at maximum power, and current at maximum power. This enhancement results in a notable 10% increase in PV module power output, from 6.58W before coating to 7.22W after coating. The observed temperature reduction is attributed to the high emissivity of the ceramic layer, measured at 0.96 using a Fluke thermal camera. Extrapolating these findings to a larger scale, calculations for a 500W coated panel show a substantial power increase of 50W in hot weather conditions. Moreover, the annual energy gain is estimated to be 87kWh, with an impressive payback time of 1.5 years. Additionally, there is a noteworthy environmental impact, with a yearly reduction of 60kg of CO_2 emissions.

Keywords: Al_2O_3 NPs; Self-cooling; Passive radiation; Photovoltaic module
Received: 06 February 2024; **Revised:** 28 March 2024; **Accepted:** 03 April 2024

1. Introduction

Despite decades of progress since the first silicon solar cell, the inherent limitations of the p-n junction architecture, as defined by the Shockley limit, constrain its maximum power output per area [1,2]. The theoretical efficiency limit of a single-junction silicon cell hovers around 33%, due to the inability to efficiently utilize all captured sunlight. This limitation arises from unabsorbed low-energy photons and thermal losses from high-energy photon absorption. In addition to the intrinsic limitations of silicon photovoltaic (PV) cell efficiency, environmental conditions contribute to additional efficiency losses, including cloud cover, dust, and temperature. The first two factors lead to a reduction in irradiance and subsequently a drop in PV module power, while the last one predominantly affects the PV voltage [3]. In extremely hot countries such as Iraq, the PV efficiency may decrease to as low as 30% of its original value. To address these challenges, a high emissivity surface can be utilized as a heat sink layer for PV panels. Inorganic metal oxide nanomaterials, previously employed in Passive Daytime Radiative Cooling Systems, offer a solution due to their high rate of infrared emission [4,5]. Previous studies have recorded a sub-ambient cooling of 2.8°C for surface cooling using a mixture of Al_2O_3, SiO_2, and Si_3N_4 nanoparticles [6]. Ongoing research efforts continue to explore various cooling methods for PV modules [7-10].

This paper presents the first attempt to deposit a high emissivity layer on the rear side of a PV module, serving as an infrared passive radiative self-cooling layer. Aluminum oxide nanoparticles blended with sodium metasilicate were chosen as the passive cooling layer in this novel approach.

Burch's equation, derived from the Shockley model of the diode, provides a tool for examining the influence of irradiance and temperature on the open-circuit voltage (V_{OC}) and short-circuit current (J_{SC}) [11].

$$I_{SC} = [I_{SCr} + K_I(T_{Panel} - T_r)]\frac{G}{G_r} \quad (1)$$

$$V_{OC} = V_{OCr} + K_V(T_{Panel} - T_r) \quad (2)$$

where T_r is the ambient temperature (standard about 25ºC), T_{Panel} is the real panel's temperature, I_{SCr} & V_{OCr} are short circuit current and open circuit voltage at the standard conditions (1000W/m^2, temperature of 25°C) respectively, K_I & K_V are the temperature coefficients respectively, G_r is the standard irradiance (1000W/m^2), and G is the real irradiance

Equation (1) reveals that the short circuit current (I_{SC}) is contingent on both temperature and irradiance, establishing a direct correlation with both T and G. In contrast, equation (2) illustrates that the open circuit voltage (V_{OC}) remains unaffected by irradiance, displaying a linear relationship solely with temperature. The source of V_{OC} lies in the built-in potential at the junction, determined by doping concentration and junction properties, with irradiance exerting no influence on these characteristics.

Essentially, as per Varshni's empirical Eq. (3), an elevated temperature induces a reduction in the silicon bandgap, resulting in an upsurge in the saturation current, commonly known as leakage current, in accordance with Shockley's model Eq. (4) [12]

$$E_g(T) = E_g(0) - \frac{\alpha T^2}{T+\beta} \quad (3)$$

$$I_S = AT^3 \exp\left(-\frac{E_g}{nkT}\right) \quad (4)$$

where $E_g(0)$ denotes the silicon bandgap at zero Kelvin, while α and β are material-specific parameters. I_S represents the saturation current (leakage current), A is the Shockley constant for silicon, E_g is the bandgap of silicon at the given temperature, n is the ideality factor of the diode, k is the Boltzmann constant, and T is the temperature in Kelvin

The open circuit voltage (V_{OC}) is logarithmically linked to the saturation current (I_S) through the following equation [13]:

$$V_{OC} = \frac{kT}{q} \ln\left[\frac{I_{SC}}{I_S}\right] \quad (5)$$

With an increase in temperature, both I_{SC} and I_S will rise, with IS (leakage current) dominating in Eq. (4). Specifically, I_S doubles in magnitude for every 10°C temperature increase. Consequently, the logarithmic component of Eq. (5) experiences a significant reduction, leading to a notable decrease in V_{OC}. Consequently, the PV power output is diminished.

The decrease in power in a PV module due to temperature is governed by the module's temperature coefficient, typically around 0.45% per degree Celsius [14]. This coefficient reflects the rate at which power decreases after the Standard Test Conditions (STC) temperature of 25°C. The power drop can be estimated using the following equation:

$$\text{Power Drop (\%)} = (T - 25) \times \text{Temp. Coef.} \quad (6)$$

where T is the PV panel temperature (which is different from the ambient temperature). The PV panel temperature is higher than the ambient temperature by about 20°C because the PV module is a good absorber and the passing current during operation heats the panel. Homer method can be used to estimate the panel's temperature compared to ambient temperature as follows [3]:

The constant A is calculated from:

$$A = (NOCT - 20)/G \quad (7)$$

where NOCT is Nominal Operating Cell Temperature, G is the radiation in W/m^2. The constant B is calculated from:

$$B = 1 - (Eff./0.9) \quad (8)$$

where Eff. is the power conversion efficiency. The panel temperature then is calculated from:

$$\textit{Panel Temp.} = \textit{Ambient Temp} + (\textit{Radiation} \times A \times B) \quad (9)$$

As an example of the Homer method, consider a PV module with a maximum power of 250W operating at an ambient temperature of 50°C. According to equations (7-9), the PV panel temperature will be 69°C, which is 20°C higher than the ambient temperature. As per Eq. (6), the power drop will be 20W, representing an 8% decrease from the STC initial value. When extrapolating this ratio to a large-scale PV system, such a power loss becomes significant. For instance, a 1MW PV system could lose 80kW of its STC energy when operating at 50°C. In extremely hot countries like Iraq, where ambient temperatures can reach as high as 70°C in June and July, corresponding to the peak electricity demand, the PV system may experience a power loss of about 25 to 30% of its STC value.

Numerous attempts have been made to mitigate the impact of temperature on PV module performance, with water-based cooling and air-based cooling being among them [15]. However, these solutions are often not economically feasible for large-scale systems. Nanomaterials, extensively studied across various applications, including PV cells, have been employed as antireflection layers, absorbent layers, and superhydrophobic layers [3]. Some nanomaterial blends exhibit an emissivity near unity. Emissivity, defined as the effectiveness of a material's surface in emitting thermal radiation, follows the Stefan-Boltzmann law, ranging from 0 (non-emitting surface) to 1 (perfect-emitting surface or a perfect black body) [16]

$$E = \sigma T^4 \quad (10)$$

where σ is the Stefan-Boltzmann constant and equals 5.67×10^{-8} W/m^2.K^4. According to this equation, a perfect black body emits 448W/m^2. This is the highest ever emissivity that any surface can emit.

2. Experimental Procedure

2.1. Materials Characterization

Aluminum oxide nanoparticles (Al_2O_3 NPs) with α-phase were procured from Changsha Santech Company, boasting a purity level of 99.99%. This material presents as a fine white powder. To ensure its quality, the powder underwent characterization using a Scanning Electron Microscope (SEM) of the Quattro S type. Emissivity measurements were conducted employing a Fluke thermal camera. The emissivity was determined by measuring the surface temperature of the layer with a Fluke Ti125 thermal camera and a thermocouple. The Fluke SmartView Software facilitated recalibration of the emissivity to align the temperature measured by the thermal camera with the temperature recorded by the thermocouple.

2.2. PV Module Characterization

In this study, a small PV module with a nominal power of 10W was employed. The module underwent testing under Standard Test Conditions (STC) and Normal Operating Cell Temperature (NOCT) conditions, facilitated by the Keyland Photovoltaic Sun Light Simulator and Solar 4000 PV Analyzer, respectively. NOCT conditions refer to the module parameters evaluated at 50°C and 800W/m^2. Figure (1) provides a visual representation of the sun

simulator utilized in the measurements. The outcomes of the module parameters are detailed in table (1).

Fig. (1) The Keyland Photovoltaic Sun Light Simulator used for STC test

2.3. Solution Preparation and Module Painting

To prepare the solution, 1mg of Al_2O_3 NPs was added to 100ml of sodium metasilicate ($Na_2SiO_3.9H_2O$). The mixture underwent blending using an ultrasonic probe sonicator with a water jacket for 5 minutes. It is important to note that an extended sonication time could lead to overheating and solidification of the solution, while a shorter duration might result in a nonhomogeneous solution. The result was a thick, homogeneous solution with a milky color, as depicted in Fig. (2).

For the application of the back coating, a regular paintbrush was utilized on the rear side of the PV panel. The process involved the application of two layers: the first layer was painted in the horizontal direction, followed by a one-hour waiting period to allow the layer to dry. Subsequently, a second layer was applied over the first one, this time in the vertical direction. This sequential application resulted in an approximately 5mm micrometer thickness of the back coating layer on the substrate of the solar modules. The coated layer was left to dry completely overnight.

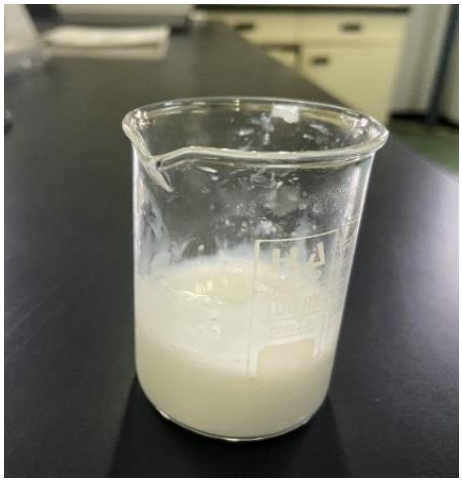

Fig. (2) The solution of the paint after 5 min probe sonicating

Figure (3) visually represents the PV module both before and after the coating process. The total rear area of the PV module is $0.25m^2$, and the coating was applied to nearly the entire area, with only a small portion near the edges left uncoated.

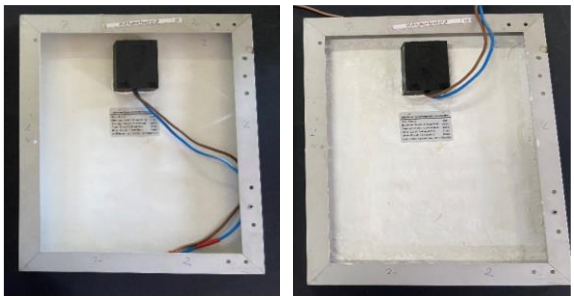

Module before Coating **Module after Coating**

Fig. (3) Rear side of the panel before and after coating with Al_2O_3 NPs

3. Results and Discussion

Figure (4) depicts the influence of average ambient temperature on both the PV output power and the surface temperature of the PV panel over the course of a year. The data presented pertains to a 250W (STC) PV panel and was gathered in Baghdad throughout the year 2018. As evident from the figure, the surface temperature of the PV panel consistently exceeds the ambient temperature, aligning with the previously mentioned Eq. (9). The decline in power as temperature rises is in accordance with the findings of Eq. (6).

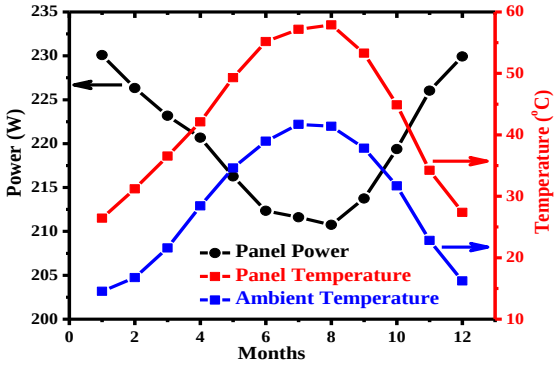

Fig. (4) The variation of PV module power with ambient over one year in Baghdad city

The SEM image of the Al_2O_3:Na_2SiO_3 blend is presented in Fig. (5a), revealing a matrix of sodium metasilicate adorned with Al_2O_3 nanoparticles. Pinholes are evident in the image, attributed to the non-homogeneity of the coated layer. Figure (5b) zooms in on the Al_2O_3 nanoparticles, showing a diverse particle size distribution ranging from 30nm to 50nm. Notably, a few particles exceed 50nm, while others are below 30nm.

For a more detailed examination of the specimens' morphological features, SEM images of native Al_2O_3 nanoparticles and modified Al_2O_3 nanoparticles were acquired (Fig. 5). The modified Al_2O_3 nanoparticles

exhibit a homogeneous dispersion, as depicted in Fig. (5a), while apparent agglomeration is observed in the image of native Al_2O_3 nanoparticles (Fig. 5b). This observation suggests that chemical or physical bonding occurs between the polarity bonds of KH-560 and hydroxide groups. The macromolecular chains grafted onto the surface of Al_2O_3 nanoparticles induce mutual exclusion and steric hindrance effects, reducing the surface free energy and effectively controlling agglomeration. These findings emphasize the crucial role of KH-560 in achieving the dispersion of Al_2O_3 nanoparticles [17].

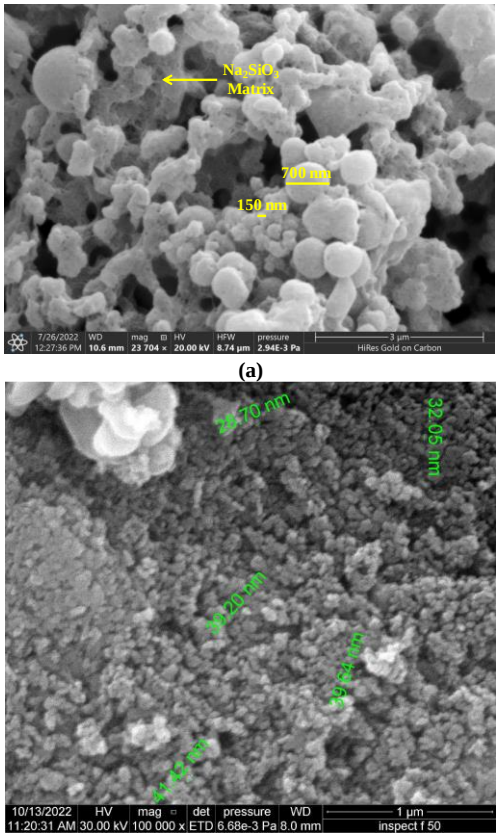

(a)

(b)

Fig. (5) SEM images of (a) Al_2O_3: Na_2SiO_3, and (b) Al_2O_3 nanoparticles

On August 30, 2021, at 12:00 PM, two PV modules were tested after being exposed to direct sunlight for one hour to allow their temperature to equalize with the ambient conditions. At the time of testing, the solar radiation and ambient temperature were 837 W/m^2 and 53°C, respectively. The uncoated rear surface of one module registered a temperature of 63°C, while the rear side of the module coated with Al_2O_3 nanoparticles exhibited a surface temperature of 58°C. This signifies a notable 5°C temperature reduction, attributed to passive cooling facilitated by the infrared emission from the nanoparticle layer induced by lattice vibration [10]. The nanoparticles absorb heat from the silicon bulk and reemit it as infrared radiation continuously, leading to the PV panel reaching an equilibrium temperature lower than that of a conventional panel. Additional contributing factors include the white color of the coating, which prevents back heating from albedo, and the increase in mass due to the layer's weight.

To calculate emissivity, a Fluke thermal camera was employed. Figure (6) displays the thermal images of the panel before and after coating. At an emissivity of 1 (perfect black body), the camera read 53.6°C, whereas for the uncoated panel, it was 58.1°C. Emissivity was determined by using a thermocouple to measure the temperature at the same surface point. The emissivity value was adjusted using SmartView Software until the temperature matched that measured by the thermocouple. At this point, the emissivity was found to be 0.96, a remarkably high value even exceeding that of black paint. This high emissivity accounts for the reduction in panel temperature compared to the uncoated counterpart. In comparison to other cooling methods, such as using phase change material as passive cooling for PV panels, which demonstrates a power increase of about 5.23% under similar conditions [18], the Al_2O_3 nanoparticle coating shows promising effectiveness.

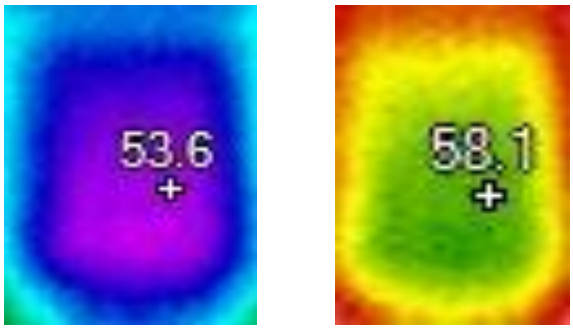

Temperature before Calibration **Temperature after Calibration**

Fig. (6) Thermal image taken by Fluke thermal camera

The IV curves of the PV panel under different conditions are presented in Fig. (7). An initial test at room temperature (RT) was conducted for comparison purposes. As depicted in the figure, the PV panel coated with Al_2O_3 nanoparticles demonstrates improved values for V_{OC} and Pm in comparison to the uncoated PV panel. However, I_{SC} shows no significant effect, as temperature predominantly influences voltage rather than current, as discussed in Eq. 5 and the subsequent paragraph. The results of the PV parameters are summarized in table (2). Notably, the coated PV panel shows a 10% increase in maximum power (P_m). This outcome holds considerable significance when considering the potential application of this technique to large-scale PV systems.

Table (2) highlights the increase in V_{OC}, V_m, I_{SC}, and I_m for the passive cooling nanocomposite paint applied to solar panels. To enhance the visibility of the results from table (2), a feasibility analysis was conducted for a 500W PV panel, as depicted in table (3). The table reveals that each coated panel can yield

an additional 50W of power. This translates to an annual energy gain of 87kWh and a reduction of 60kg of CO_2 emissions per year. With a coating cost of $12 per module, the payback period for this investment is a mere 1.5 years. This underscores the economic viability and potential environmental benefits of implementing the coating on solar panels.

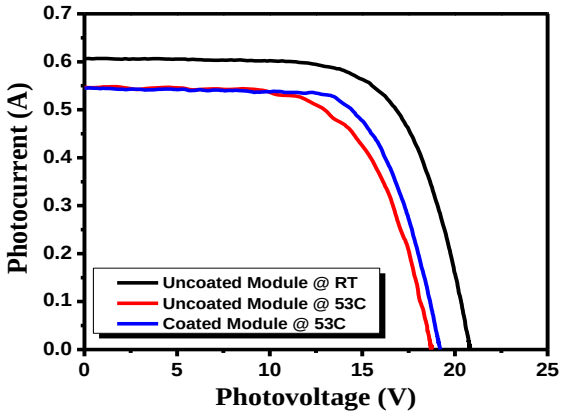

Fig. (7) The forth quadrant IV curves under illumination

Table (3) Feasibility estimation on 500W PV panel coated with Al_2O_3 NPs

Power Difference	50W
Panel Area	$2m^2$
Energy Gain in One Year	87kWh
Paint Cost	$12
Electricity Bill Price	120 ID/kWh
Yearly Profit	$7.5
Payback Time	1.5 Year
CO_2 Avoided per Year	60kg

4. Conclusions

Passive radiative self-cooling systems employing nanoparticles, such as Al_2O_3 NPs, emerge as a practical and economical solution for enhancing the efficiency of PV cooling systems when compared to conventional solar modules. In contrast to alternative methods, such as water cooling, this approach stands out as a self-cooling technique that eliminates the need for water or energy-consuming components like pumps or wipers. The method proves highly effective, inducing a substantial reduction in PV module temperature. Its efficiency and simplicity make it a promising avenue for improving the performance of solar panels.

Acknowledgment

The Corporation of Research and Industrial Development is thankful for the logistic support provided.

References

[1] D.M. Chapin, C.S. Fuller and G.L. Pearson, "A new silicon p-n junction photocell for converting solar radiation into electrical power, *J. Appl. Phys.*, 25(5) (1954) 676–677.

[2] W. Shockley and H.J. Queisser, "Detailed Balance Limit of Efficiency of p-n Junction Solar Cells," *J. Appl. Phys.*, 32(3) (1961) 510–519.

[3] S.K. Abdulridha, S.A. Tuma and O.A. Abdulrazzaq, "Study of the Partial Shading Effect on the Performance of Silicon PV Panels String," *J. Appl. Sci. Nanotechnol.*, 1(1) (2021) 32–42.

[4] F. Moreno et al., "Evaluating the efficiency of utilizing selectively optimized metamaterial nanostructures for passive radiative cooling of5t5 satellites and components," *PAM Rev. Energy Sci. Technol.*, 6 (2019) 110–123.

[5] Y. Zou et al., "Al_2O_3/reduced graphene oxide double-layer radiative coating for efficient heat dissipation," *Mater. Des.*, 157 (2018) 130–140.

[6] R. Harahap and S. Suherman, "Active versus passive cooling system in increasing solar panel output," Procedia Environmental Science, *Eng. Manag.*, 8(1) (2021) 157-166.

[7] S. Wu and C. Xiong, "Passive Cooling Technology for Photovoltaic Panels for Domestic Houses," *Int. J. Low-Carbon Technol.*, 9(2) (2013) 118-126.

[8] E. Kozak-Jagieła, P. Cisek and P. Ocłoń, "Cooling techniques for PV panels: A review", *Scientiae Radices*, 2 (2023) 47-68.

[9] A.M. Elbreki et al., "Experimental and economic analysis of passive cooling PV module using fins and planar reflector", *Case Studies Therm. Eng.*, 23 (2021) 100801.

[10] D. Chae et al., "Spectrally Selective Nanoparticle Mixture Coating for Passive Daytime Radiative Cooling," *ACS Appl. Mater. Interfaces*, 13(18) (2021) 21119–21126.

[11] M. Arnaout, W. Salameh and A. Assi, "Impact of solar radiation and temperature levels on the variation of the series and shunt resistors in photovoltaic modules", *Int. J. Res. Eng. Technol.*, 5(3) (2016) 295-301.

[12] S.M. Sze and K.K. Ng, **"Physics of Semiconductor Devices"**, 3rd ed., John Wiley & Sons, Inc. (2007).

[13] M. Rudan, **"Physics of Semiconductor Devices"**, 3rd ed., John Wiley & Sons, Inc. (2015).

[14] A. Descoeudres et al., "Silicon Heterojunction Solar Cells: Towards Low-cost High-Efficiency Industrial Devices and Application to Low-concentration PV," *Energy Procedia*, 77 (2015) 508–514.

[15] Y.M. Irwan et al., "Indoor Test Performance of PV Panel through Water Cooling Method," *Energy Procedia*, 79 (2015) 604–611.

[16] K. Tang et al., "A Thermal Radiation Modulation Platform by Emissivity Engineering with Graded Metal–Insulator Transition," *Adv. Mater.*, 32(36) (2020) 1907071.

[17] T. Luo et al., "Study of Surface Modification of Al_2O_3 Nanoparticles with KH-560", *Asian J. Chem.*, 25(12) (2013) 6777-6779.

[18] A. Al Miaari and H. Muhammad Ali, "Technical method in passive cooling for photovoltaic panels using phase change material", *Case Studies Therm. Eng.*, 49 (2023) 103283.

Table (1) PV module parameters of the used panel

Condition	V_{oc} (V)	I_{sc} (A)	V_m (V)	I_m (A)	P_m (W)	Effic. (%)	FF	Rad. (W/m²)	Temp. (°C)
STC	21.38	0.52	17.43	0.47	8.16	3.2	0.73	1000	25
NOCT	18.89	0.49	12.96	0.32	4.20	1.6	0.45	800	50

Table (2) The PV parameters of the PV module before and after coating

Condition	V_{oc} (V)	I_{sc} (A)	V_m (V)	I_m (A)	P_m (W)	Effic. (%)	FF	Rad. (W/m²)	Amb. Tem. (°C)	Surf. Tem. (°C)
Reference @ 35°C	20.83	0.60	16.04	0.53	8.57	3.4	0.68	870	35	35
Before Coating	18.65	0.54	14.21	0.45	6.39	2.5	0.62	837	53	63
After Coating	19.20	0.54	14.35	0.50	7.22	2.8	0.69	837	53	58

